ChemComm

Design of Phase-Transition Molecular Solar Thermal Energy Storage Compounds: Compact Molecules with High Energy Densities

Journal:	*ChemComm*
Manuscript ID	CC-COM-07-2021-003742.R1
Article Type:	Communication

COMMUNICATION

Design of Phase-Transition Molecular Solar Thermal Energy Storage Compounds: Compact Molecules with High Energy Densities

Received 00th January 20xx,
Accepted 00th January 20xx

DOI: 10.1039/x0xx00000x

Qianfeng Qiu, Mihael A. Gerkman, Yuran Shi, and Grace G. D. Han*

A series of compact azobenzene derivatives were investigated as phase-transition molecular solar thermal energy storage compounds that exhibit maximum energy storage densities around 300 J/g. The relative size and polarity of the functional groups on azobenzene were manifested to significantly influence the phase of isomers and their energy storage capacity.

Molecular solar thermal (MOST) energy storage compounds that photo-isomerize to store solar photon energy in their metastable isomers have emerged as a complementary solar harvesting method to photovoltaics and artificial photosynthesis, enabling a closed-system energy storage and a controlled release of thermal energy. Several classes of photoswitches, particularly norbornadienes,[1,2] dihydroazulenes,[3,4] fulvalene dimetal complexes,[5,6] and azoarenes,[2,7] have been investigated for MOST applications, among other conventional or emerging switches such as spiropyrans,[8] hydrazones,[9] and donor-acceptor Stenhouse adducts.[10] Various design strategies have been developed to increase their energy storage densities around or above 300 J/g and accomplish the storage cycle in a condensed phase, in pursuit of realizing a practical application of such systems.[11,12]

One of the major strategies incorporates the simultaneous phase transition and photo-isomerization, which leverages the latent heat storage in the system to increase the total energy storage beyond the isomerization enthalpy of a photoswitch.[13–16] In particular, asymmetric azobenzenes or heteroazoarenes functionalized with long alkyl chains have been largely studied as phase-transition MOST (PT-MOST) materials, primarily due to their structural resemblance to conventional organic phase change materials (PCMs) and the favourable formation of crystalline *E* isomers and liquid *Z* isomers at room temperature.[16–20] However, these heavy molecules are generally compromised by their low gravimetric energy densities, which limits their deployment for practical energy storage devices and applications. Previous investigations on such materials have mostly focused on the impact of alkyl chain lengths (C_6 to C_{15}) on the latent heat storage as well as that of heteroarene structures on the half-lives of *Z* isomers which determine the energy storage period.

On the other hand, pristine azobenzene and most azobenzene derivatives without alkyl chains remain unexplored for their potential as PT-MOST materials due to their dissimilar structures from the conventional organic PCMs.[20] Only *p*-methoxy-functionalized azobenzene has been recently studied as a compact PT-MOST.[21] Other functionalized azobenzenes have been primarily investigated for their fundamental optical switching properties in solutions or the associated isomerization enthalpies.[22–25] The translation of such solution-state properties to condensed phases has important implications for developing photon energy storage devices with high energy densities, which is yet to be elucidated.

Herein, we investigate a set of compact azobenzene derivatives, with small functional groups of varied size and polarity, in order to unravel design principles for achieving an efficient PT-MOST with a high energy density. As illustrated in **Fig. 1**, a series of *p*-functionalized azobenzene derivatives were prepared such that the Hammett constants (σ) of the functional groups range from -0.27 to 0.78, varying electron-donating and -withdrawing properties.[26] The absolute σ values show a linear correlation with the dipole moments of *E* isomers, obtained by DFT calculations (**Fig. S1** and **Table S1**). Nine compounds are listed and numbered in the order of increasing values of σ. Their optical absorption spectra measured in solution show the reversible photoswitching between *E* and *Z*, induced by the UV and visible light irradiations (**Fig. S2**). In solid state, as illustrated in **Fig. 1**, the initial *E* isomers absorb heat of fusion (*i.e.* melting enthalpy) to form a molten state and subsequently absorb UV to isomerize to *Z* forms. The photostationary state (PSS) ratios of *E* and *Z* isomers acquired in solution and in solid state are different, as summarized in **Table S2**. The non-planar *Z* isomers generally form a liquid or a supercooled liquid phase upon

Department of Chemistry, Brandeis University, 415 South Street, Waltham, MA 02453, USA.
E-mail: gracehan@brandeis.edu
Electronic Supplementary Information (ESI) available: methods, synthesis, UV-Vis spectra, DSC plots, kinetic analysis, film studies, DFT results. See DOI: 10.1039/x0xx00000x

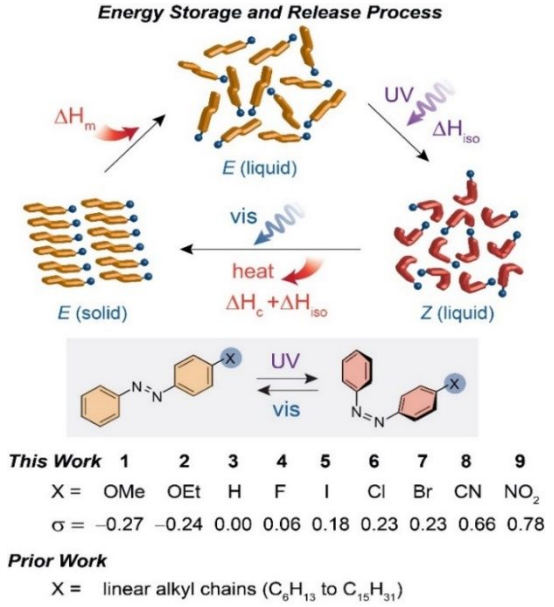

Fig. 1 Phase transition and photo-isomerization process of azobenzene derivatives that store energy in a liquid state and release it upon optical triggering by visible light irradiation. The list of the investigated azobenzene derivatives and the corresponding Hammett constants.

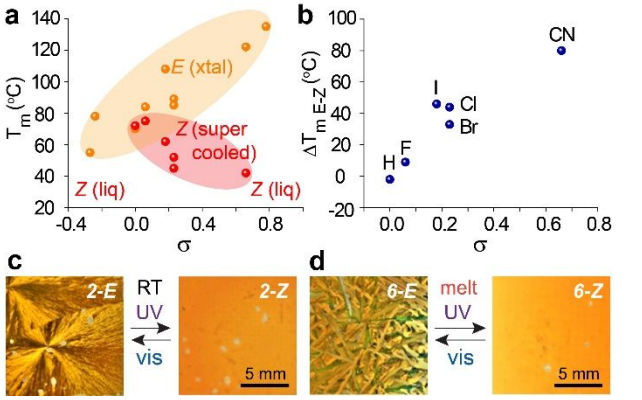

Fig. 2 (a) Melting points and phase characteristic of E and Z isomers of all compounds bearing functional groups with corresponding Hammett constants. (b) The melting point difference between respective E and Z isomers of each compound. (c, d) Optical microscope images of E and Z isomers of 2 and 6.

melting and subsequent cooling. The *Z* isomers that are still crystalline at room temperature typically exhibit lower melting points than those of *E* isomers. These phase difference between the *E* and *Z* isomers leads to the additional heat storage in such compounds compared to the mono-phase MOST materials. The *Z* liquid (or supercooled liquid) phase is then triggered by visible light irradiation to undergo a simultaneous crystallization and reverse isomerization, releasing the crystallization enthalpy (ΔH_c of *E* isomer) and the *Z*-to-*E* isomerization enthalpy (ΔH_{iso}).

Thus, significant phase difference between each isomer is critical for increasing the overall energy storage density in PT-MOST systems.[7] **Fig. 2a** shows the melting points of *E* and *Z* isomers of each compound. All of the *E* isomers (marked orange) were crystalline, exhibiting clear melting and crystallization points in differential scanning calorimetry (DSC) measurements (**Fig. S3**). The phase of *Z* isomers, on the other hand, is highly dependent on the *p*-substituent (see **Fig. S3** for DSC thermograms, **Table S3** for all thermal parameters). We note that *Z* isomers were prepared in solution and dried to measure their thermal properties by DSC. The *Z* isomer of pristine azobenzene **3** is crystalline at room temperature, melts and crystallizes upon heating and cooling, similar to the *E* isomer, while displaying a significant supercooling by 70 °C. The *Z* isomers of **4-8** bearing halides and a nitrile group are crystalline at room temperature, melt between 40 and 80 °C, but do not crystallize upon cooling down to −90 °C. These compounds are relatively stable as liquid at room temperature after pre-melting, and the supercooled liquid *Z* isomers cold-crystallize over time. The *Z* isomers of **1** and **2** exhibit stable liquid phases in the absence of any melting or crystallization behaviours upon heating and cooling. The distinct phases, *i.e.* liquid as *Z* and crystalline as *E*, of these compounds are highly promising conditions for PT-MOST compounds. Compound **9** achieves a low *Z* ratio (47%) in solution under UV irradiation, and the DSC measurement of the *E* and *Z* mixture at the PSS does not display any melting or crystallization of the *Z* isomer, which likely infers the liquid phase of *Z*. The optical absorption spectra of compounds in solid and condensed liquid are shown in **Fig. S4**.

For compounds **3-8**, which show different melting points for *E* and *Z* isomers, the gap between the melting points ($\Delta T_{m\ E\text{-}Z}$) is indicative of the phase difference between each isomer (**Fig. 2b**). For the pristine azobenzene, $\Delta T_{m\ E\text{-}Z}$ is negligible, showing similar phase behaviour between *E* and *Z* isomers. As the Hammett constant increases across the series of compounds, the $\Delta T_{m\ E\text{-}Z}$ also linearly increases. This results from the substantially increased melting points of polar *E* isomers and decreased melting point of corresponding *Z* isomers (**Fig. 2a**). **Fig. 2c** shows the optically-induced phase transition of **2**, substituted with an EtO group, between the crystalline *E* and liquid *Z* isomers, reversibly achieved at the room temperature by UV and visible light irradiation. Compound **1** with a *p*-MeO substitution also exhibits the direct phase transition by UV, without pre-melting, as previously reported.[21] This is in contrast to other compounds **3-9** that do not photoswitch in their crystalline phase at room temperature and require pre-melting for UV-induced *E*-to-*Z* switching to occur, according to the diagram in **Fig. 1** and exemplified as optical images of **6** in **Fig. 2d**. For all compounds, once the stable liquid *Z* is acquired, the heat release can be triggered by the visible light irradiation, notably with 430 nm or 590 nm.

The total energy stored in PT-MOST compounds is a sum of latent heat stored in the liquid phase and isomerization energy stored in *Z* isomers. In order to evaluate the potential of each compound for PT-MOST applications in condensed phases, we primarily compare their gravimetric energy densities (J/g), rather than molar storage capacity (kJ/mol; **Table S4**), focusing on identifying the candidates that exhibit energy densities near or exceeding 300 J/g, when completely isomerized. The melting and crystallization enthalpies (ΔH_m and ΔH_c) of compounds are summarized in **Fig. 3a**, which shows a generally increasing trend of both quantities as a function of Hammett constant, except for molecules with heavy substituents (Br and I). This signifies the necessity for reducing the molecular weight of photoswitches.[27] The negative correlation between the latent heat and molecular weight is highlighted in **Fig. S5** along with

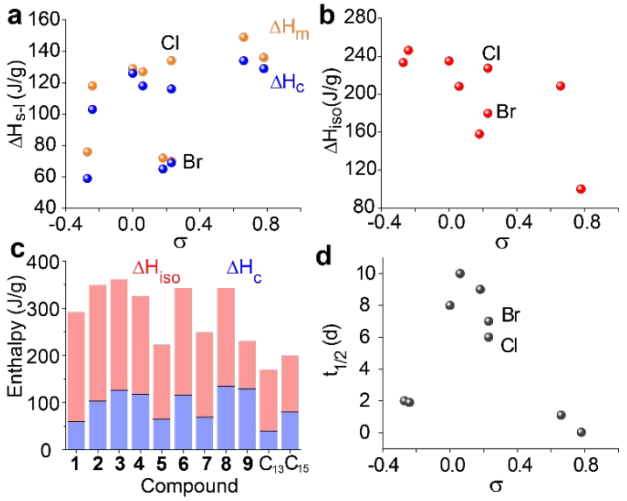

Fig. 3 (a) Melting and crystallization enthalpies of *E* isomers. Cl and Br derivatives with the identical Hammett constant are labelled for clarification. (b) Isomerization enthalpies of all compounds. (c) The total energy storage densities shown as a sum of maximum isomerization enthalpy and *E* isomer crystallization enthalpy of **1-9** and two reported compounds with longer alkoxy chains on the 4-position of azobenzene. (d) Half-lives of Z isomers.

the positive correlation between the dipole moment of compounds and their melting points. Compounds **1** and **2** exhibit lower latent heat storage than **6**, despite similar molecular weight, due to the weaker π–π interactions between aromatic cores in a crystalline phase. This corroborates the more facile photo-switching of **1** and **2** in solid at room temperature than **6**, as illustrated in **Fig. 2c** and **2d**.

The gravimetric isomerization enthalpy (ΔH_{iso}) of each compound was obtained by the DSC analysis of *Z* isomers, prepared by the irradiation in solution, under thermal activation conditions. We report the energy release from 100% *Z* of each compound (**Table S5**) to gauge its potential as a MOST compound in the optimized photoswitching conditions (wavelength, optical power, irradiation time, etc.). The ΔH_{iso} values are the lowest for **5**, **7**, and **9**, due to the heavy substituents (**5** and **7**) and the rapid loss of *Z* isomer (**9**). Determining an accurate %*Z* of **9** is challenging, due to the extremely facile thermal reversion of *Z* at room temperature, which also leads to the underestimation of ΔH_{iso} measured by DSC. Furthermore, the overlapping features of *Z*-to-*E* thermal reversion and *E* isomer crystallization in DSC analysis exacerbate the difficulty in the precise measurement of ΔH_{iso}.[28] However, the rest of compounds show high ΔH_{iso} in the range of 200-250 J/g. The exothermic features from the *Z*-to-*E* thermal reversion are shown in **Fig. S6**. The ΔH_{iso} are generally greater than the latent heat as shown in **Fig. 3c**, while the latent heat component is essential in achieving the total energy densities ~300 J/g.[11,12] A substantial number of compact compounds in the series studied (**1**, **2**, **3**, **4**, **6**, and **8**) fulfil the figure of merit, in clear contrast to the previously reported azobenzenes bearing long *p*-alkoxy chains (C_{13} and C_{15}).[19] Other azoarene compounds modified with alkyl chains (C_6 to C_{13}) for achieving PT-MOST generally display the energy densities in the range of 150-200 J/g, as a result of the high molecular weight.[16,18] They are, however, designed to improve different parameters of PT-MOST, notably a long heat storage period (*i.e.* high stability of *Z*

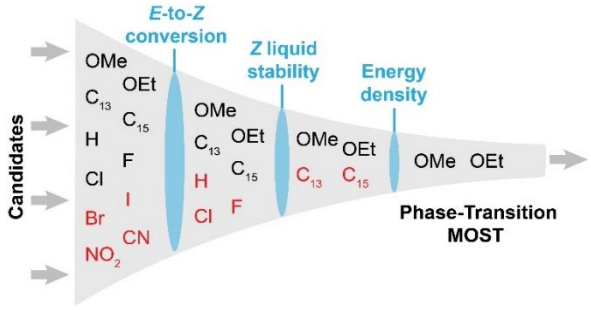

Fig. 4 Selection process of PT-MOST compounds.

liquid), absorption of visible light for *E*-to-*Z* isomerization, and storage of *Z* liquid at sub-zero temperatures, all of which expands the utility of this unique class of energy storage materials. A group of alkyl-functionalized arylazopyrazoles recently reported by Li and Moth-Poulsen showed an exceptional energy storage above 300 J/g,[17] while the rest of alkyl-substituted azoarenes demonstrated the concept of PT-MOST without much optimization of energy densities.

Lastly, the half-lives of *Z* isomers are illustrated in **Fig. 3d**, which influences the storage time of *Z* liquid at room temperature.[29] For diurnal energy storage applications, particularly for harnessing solar heat and photon, the half-lives greater than 1 day are desired, which makes it difficult to use **9** with an exceptionally short half-life of 58 min. The kinetic analysis of the *Z*-to-*E* reversion for all compounds and the relevant thermal activation energy are shown in **Fig. S7** and **Table S6**. The volcano plot of the half-life vs. Hammett constant has been observed for azobenzene derivatives, as a result of the facilitated reversion of *Z* to *E* induced by the strong electron donating or withdrawing groups.[30]

Fig. 4 summarizes the process of selecting promising PT-MOST compounds from a set of candidate photoswitches, based on the performance metrics and the relevant optical and thermal parameters. The first metric is the successful *E*-to-*Z* conversion in condense phases (**Table S2**), achieved by the UV irradiation either at room temperature or an elevated temperature at which molten or supercooled *E* isomers exist. The compounds **5**, **7**, **8**, and **9** exhibit high melting points (85–135 °C) and crystallization points (74–119 °C) with marginal supercooling as *E* isomers (**Table S3**), thus the molten *E* isomers at such high temperatures above 74 °C cannot effectively switch to *Z* under UV irradiation due to the facile thermal *Z*-to-*E* reversion. Since a substantial ratio of *Z* isomer (>50%) in the condensed phase cannot be achieved, the effective energy storage in *Z* liquid is not viable, leading to the elimination of the compounds from the pool of candidate materials.

All other compounds that show effective UV switching to *Z* isomers (>50% *Z*) in condensed phases are then inspected for the stability of *Z* liquid state. This can be achieved if *Z* isomers form a liquid phase at room temperature (compounds **1**, **2**, C_{13}, and C_{15}) or a stable supercooled liquid phase.[16,18,31,32] Compounds **3** and **6** containing 53% and 55% of *Z* isomer upon UV irradiation in condensed phases could not retain a liquid phase over 1 day at room temperature (**Fig. S8**), due to the crystallization of considerable *E* isomers. Compound **4**, despite the high %*Z* (75%) obtained by UV irradiation at ~60 °C in

condensed liquid, gradually crystallized upon the cooling to room temperature, susceptible to a facile cold-crystallization. The unsatisfactory liquid phase stability of **3**, **4**, and **6** thus significantly limits their utility for MOST applications.

Finally, compounds **1** and **2** along with previously reported C_{13} and C_{15} derivatives[19] that are capable of achieving a facile *E*-to-*Z* conversion under UV and forming stable liquid (92% and 80% *Z*; **Fig. S8**) were evaluated for MOST application based on their energy storage densities. Large degrees of maximum energy storage at 349 J/g and 292 J/g were achieved with **2** and **1**, respectively, and the liquid phase is effectively triggered by visible light to crystallize and release the stored energy (**Fig. S9**, **S10**). The *Z* half-lives of ~2 days allow for the diurnal storage of *Z* liquid phase and thermal energy in these compounds. We also demonstrated the reversible isomerization and phase transition of compound **2** at 200 mg scale under the alternating irradiation at 365 nm and 590 nm (**Fig. S11**). Although the C_{13} and C_{15} derivatives present comparable optical and thermal characteristics to those of **1** and **2**, their high molecular weights lower the gravimetric energy densities below 200 J/g, rendering them less desirable for practical MOST applications.[19]

In conclusion, we find a strong correlation between the efficacy of azobenzene-based PT-MOST compounds and their *p*-substituents, particularly their polarity and size. Highly electron-donating or -withdrawing groups afford a large difference between the phase of *E* (crystalline) and *Z* (liquid) isomers, while decreasing the half-lives of the *Z* isomers. Electron-donating groups, MeO and EtO, increase ΔH_{iso} while lowering the latent heat (ΔH_c) of azobenzene derivatives. ΔH_c is largely dependent on the shape and size of substituents that influence the packing of molecules and weight of compound. Most importantly, the photo-switchability of *E* isomers in condensed phases and subsequent formation of stable *Z* liquid determine the viability of the PT-MOST energy storage. From this study, we find that two compounds **1** and **2** bearing small substituents (MeO and EtO) are capable of storing ~300 J/g or more as a result of the compact structure and polar nature of the substituents, enabling the facile photon and heat storage through phase transition and reversible photo-isomerization. We note that UV-absorbing azobenzene derivatives generally have a limited light penetration depth (~μm) due to the large overlap of absorbance between *E* and *Z* in UV range. Also, these molecules can only harness a small fraction (4.5%) of UV in solar spectrum.[16] Therefore, developing design principles for the spectral separation of *E* and *Z* isomers and red-shifting their absorption to visible light range will be critical to achieve direct solar harvesting and efficient energy storage in large-scale PT-MOST compounds.

This work was supported by Brandeis NSF MRSEC, Bioinspired Soft Materials (DMR-2011486) and Brandeis SPROUT award (2019–042). Y.S. thanks 2020 Division of Science SURF and Tema Nemtzow'79 and Professor Kraig Steffen Student Research Endowment Fellowship.

Conflicts of interest

There are no conflicts to declare.

Notes and references

1 J. Orrego-Hernández, A. Dreos and K. Moth-Poulsen, *Acc. Chem. Res.*, 2020, **53**, 1478–1487.
2 A. Lennartson, A. Roffey and K. Moth-Poulsen, *Tetrahedron Lett.*, 2015, **56**, 1457–1465.
3 M. Brøndsted Nielsen, N. Ree, K. V. Mikkelsen and M. Cacciarini, *Russ. Chem. Rev.*, 2020, **89**, 573–586.
4 A. Vlasceanu, M. Cacciarini and M. B. Nielsen, *Tetrahedron*, 2018, **74**, 6635–6646.
5 Y. Kanai, V. Srinivasan, S. K. Meier, K. P. C. Vollhardt and J. C. Grossman, *Angew. Chemie - Int. Ed.*, 2010, **49**, 8926–8929.
6 K. Moth-Poulsen, D. Ćoso, K. Börjesson, N. Vinokurov, S. K. Meier, A. Majumdar, K. P. C. Vollhardt and R. A. Segalman, *Energy Environ. Sci.*, 2012, **5**, 8534–8537.
7 L. Dong, Y. Feng, L. Wang and W. Feng, *Chem. Soc. Rev.*, 2018, **47**, 7339–7368.
8 R. Klajn, *Chem. Soc. Rev.*, 2014, **43**, 148–184.
9 B. Shao and I. Aprahamian, *Chem*, 2020, **6**, 2162–2173.
10 H. Nie, J. L. Self, A. S. Kuenstler, R. C. Hayward and J. Read de Alaniz, *Adv. Opt. Mater.*, 2019, **7**, 1900224.
11 M. Mansø, A. U. Petersen, Z. Wang, P. Erhart, M. B. Nielsen and K. Moth-Poulsen, *Nat. Commun.*, 2018, **9**, 1–7.
12 V. A. Bren', A. D. Dubonosov, V. I. Minkin and V. A. Chernoivanov, *Russ. Chem. Rev.*, 1991, **60**, 451–469.
13 M. A. Gerkman and G. G. D. Han, *Joule*, 2020, **4**, 1621–1625.
14 K. Ishiba, M. A. Morikawa, C. Chikara, T. Yamada, K. Iwase, M. Kawakita and N. Kimizuka, *Angew. Chemie - Int. Ed.*, 2015, **54**, 1532–1536.
15 G. D. Han, S. S. Park, Y. Liu, D. Zhitomirsky, E. Cho, M. DincĂ and J. C. Grossman, *J. Mater. Chem. A*, 2016, **4**, 16157–16165.
16 Y. Shi, M. A. Gerkman, Q. Qiu, S. Zhang and G. G. D. Han, *J. Mater. Chem. A*, 2021, **9**, 9798–9808.
17 Z. Y. Zhang, Y. He, Z. Wang, J. Xu, M. Xie, P. Tao, D. Ji, K. Moth-Poulsen and T. Li, *J. Am. Chem. Soc.*, 2020, **142**, 12256–12264.
18 M. A. Gerkman, R. S. L. Gibson, J. Calbo, Y. Shi, M. J. Fuchter and G. G. D. Han, *J. Am. Chem. Soc.*, 2020, **142**, 8688–8695.
19 H. Liu, Y. Feng and W. Feng, *Compos. Commun.*, 2020, **21**, 100402.
20 M. M. Kenisarin, *Sol. Energy*, 2014, **107**, 553–575.
21 J. Hu, S. Huang, M. Yu and H. Yu, *Adv. Energy Mater.*, 2019, **9**, 1–10.
22 S. C. Cheng, K. J. Chen, Y. Suzaki, Y. Tsuchido, T. S. Kuo, K. Osakada and M. Horie, *J. Am. Chem. Soc.*, 2018, **140**, 90–93.
23 L. Wang, A. Ishida, Y. Hashidoko and M. Hashimoto, *Angew. Chemie - Int. Ed.*, 2017, **56**, 870–873.
24 M. Schönberger and D. Trauner, *Angew. Chemie - Int. Ed.*, 2014, **53**, 3264–3267.
25 M. Volgraf, P. Gorostiza, S. Szobota, M. R. Helix, E. Y. Isacoff and D. Trauner, *J. Am. Chem. Soc.*, 2007, **129**, 260–261.
26 C. Hansch, A. Leo and R. W. Taft, *Chem. Rev.*, 1991, **91**, 165–195.
27 Q. Qiu, Y. Shi and G. G. D. Han, *J. Mater. Chem. C*, , DOI:10.1039/d1tc01472b.
28 C. Knie, M. Utecht, F. Zhao, H. Kulla, S. Kovalenko, A. M. Brouwer, P. Saalfrank, S. Hecht and D. Bléger, *Chem. - A Eur. J.*, 2014, **20**, 16492–16501.
29 C.-L. Sun, C. Wang and R. Boulatov, *ChemPhotoChem*, 2019, **3**, 268–283.
30 G. Angelini, N. Canilho, M. Emo, M. Kingsley and C. Gasbarri, *J. Org. Chem.*, 2015, **80**, 7430–7434.
31 G. G. D. Han, J. H. Deru, E. N. Cho and J. C. Grossman, *Chem. Commun.*, 2018, **54**, 10722–10725.
32 H. Liu, J. Tang, L. Dong, H. Wang, T. Xu, W. Gao, F. Zhai, Y. Feng and W. Feng, *Adv. Funct. Mater.*, 2021, **31**, 2008496.

